infrastructures

Article

Predictive Stress Modeling of Resilient Modulus in Sandy Subgrade Soils

Tadas Tamošiūnas * and Šarūnas Skuodis

Department of Reinforced Concrete Structures and Geotechnics, Vilnius Gediminas Technical University, 10223 Vilnius, Lithuania
* Correspondence: tadas.tamosiunas@vilniustech.lt

Abstract: The mechanical properties of pavement materials are crucial to the design and performance of flexible pavements. One of the most commonly used measures of these properties is the resilient modulus (E_r). Many different models were developed to predict the resilient modulus of coarse soils, which are based on the states of stresses and the physical and mechanical properties of the soil. The unconsolidated unsaturated drained cyclic triaxial tests were performed for three variously graded and three well-graded sand specimens to determine the resilient modulus, and to perform predictive modeling using the K-θ, Rahim and George, Uzan, and Universal Witczak models. Obtained E_r values directly depended on the confining pressure and deviatoric stress values used during the test. The Octahedral Shear Stress (OSS) model, proposed by the authors of the paper, predicts the resilient modulus with a coefficient of determination (R^2) ranging from 0.85 to 0.99. The advantage of the model is the use of small-scale data tables, meaning fixed K_1 and K_2 regression coefficients, and it can be assigned to a specific specimen type without the need to determine them using the specific deviatoric and confining stresses.

Keywords: resilient modulus; predictive models; variously graded sand; well-graded sand; cyclic triaxial test; regression coefficients; octahedral shear stress; bulk stress

Citation: Tamošiūnas, T.; Skuodis, Š. Predictive Stress Modeling of Resilient Modulus in Sandy Subgrade Soils. *Infrastructures* **2023**, *8*, 29. https://doi.org/10.3390/infrastructures8020029

Academic Editor: Tatiana García-Segura

Received: 26 January 2023
Revised: 2 February 2023
Accepted: 6 February 2023
Published: 8 February 2023

1. Introduction

The mechanical properties of pavement materials are crucial to the design and performance of flexible pavements. One of the most commonly used measures of these properties is the resilient modulus (E_r) [1–3]. It can be determined for sandy subgrade [4–6] and clayey subgrade [7–9].

The resilient modulus (E_r) is a measure of the ability of a material to resist deformation under repeated loading. It is commonly used in the design of flexible pavements, as it provides a measure of the stiffness of the pavement material and its ability to resist rutting and fatigue [10,11].

The resilient modulus (E_r) of a material is affected by several factors, such as the type and amount of loading, the moisture content of the material, and the temperature [12,13].

To determine the resilient modulus, cyclic triaxial pressure tests are performed in the laboratory. It is difficult to perform these tests since qualified specialists are needed. Also, the tests take quite a long time and the equipment for performing such tests is expensive [14]. For these and other reasons, resilient modulus predictive models have been developed which allow modulus values to be determined without cyclic triaxial testing [15–17].

The purpose of this research work is to verify the accuracy of commonly used resilient modulus prediction models by relating their results to the experimentally determined resilient modulus of sandy soils, and also, to propose a more accurate model for forecasting sandy soils modulus values.

2. Materials and Methods

2.1. Test Procedure

To determine the resilient modulus (E_r), the isotropic unconsolidated unsaturated drained cyclic triaxial tests were performed using a Wille Geotechnik dynamic triaxial apparatus, according to the low-stress test program (method B) provided in EN 13286-7:2004 [2], which was slightly adjusted using confining stress from 20 kPa to 70 kPa (Figure 1), and the minimum value of the deviator was fixed at the limit of 10 kPa due to the limitations of the test apparatus. The maximum deviator stress and the number of cycles for a particular state of specimen loading are provided in Figure 1. The loadings of the specimen were performed at a frequency of 1 Hz with data recording intervals ranging from 100 to 150 times per second. The dimensions of the samples were 100 mm in diameter and 200 mm in height.

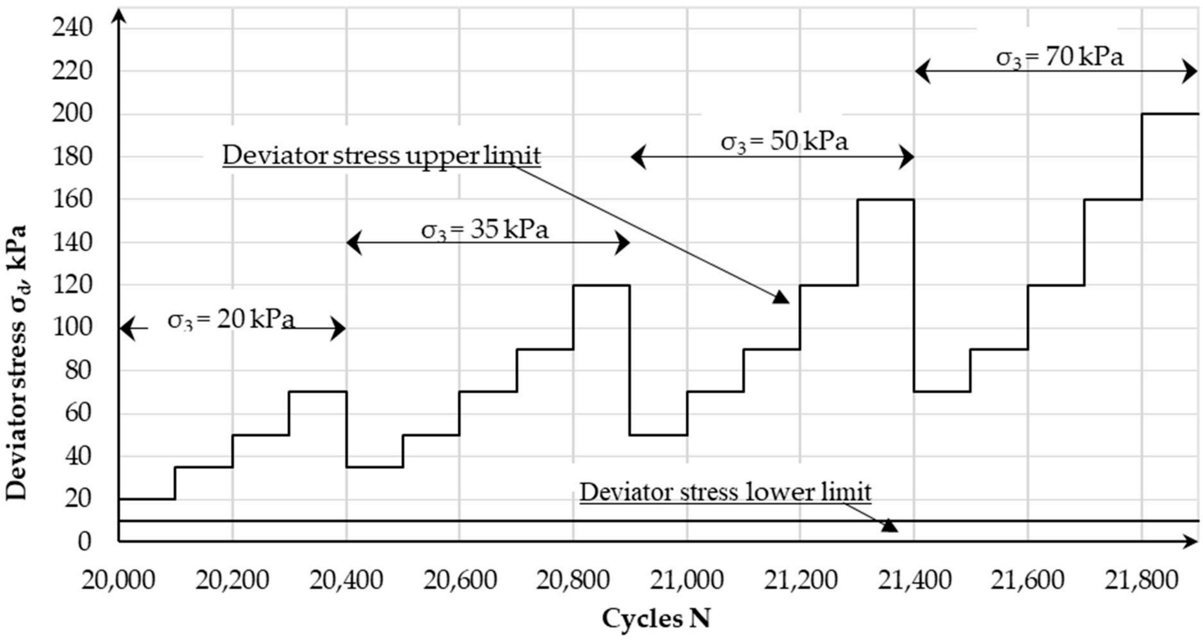

Figure 1. Test program—stress levels for the determinations of resilient behavior of soil specimens.

At the beginning of the tests, conditioning of specimens was performed with 20,000 periodic cyclic loadings at the same frequency of 1 Hz with variable stress deviator ranging from 10 to 200 kPa.

The resilient modulus was determined according to [18] and the formula given in EN 13286-7:2004 [2]:

$$E_r = \frac{\sigma_1^{r^2} - \sigma_1^r \sigma_3^r - 2\sigma_3^{r^2}}{\sigma_1^r \varepsilon_1^r + \sigma_3^r \varepsilon_1^r - 2\sigma_3^r \varepsilon_3^r} \quad (1)$$

where $\sigma_1{}^r$ is residual axial stress, $\sigma_3{}^r$ is residual radial stress, $\varepsilon_1{}^r$ is residual or restored axial relative deformation determined using displacement values from two vertical linear variable differential transformers (LVDTs), and $\varepsilon_3{}^r$—residual or restored radial relative deformation determined using displacement value from radial LVDT (Figure 2).

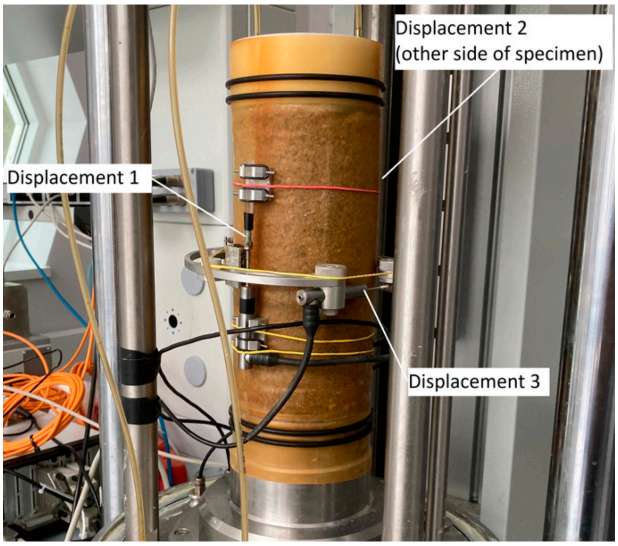

Figure 2. Specimen with attached mounted LVDTs before the start of cyclic triaxial test.

Resilient or recovered axial strain ($\varepsilon_1{}^r$) is determined by dividing resilient axial displacement at cycle N, defined as the displacement during the unloading part of the cycle (between the point where the applied stresses are maximum and the end of the cycle) from the gauge length for axial displacement (Displacement 1 and 2, see Figure 2). Resilient or recovered radial strain is determined by dividing resilient radial displacement at cycle N, defined as the displacement during the unloading part of the cycle, from the gauge length for radial displacement (Displacement 3, see Figure 2). Axial displacement was determined using two LVDTs, radial—one LVDT (Figure 2). The example determination of values of displacements at the maximum deviator stress and the last values of displacement during one cycle can be seen in Figure 3.

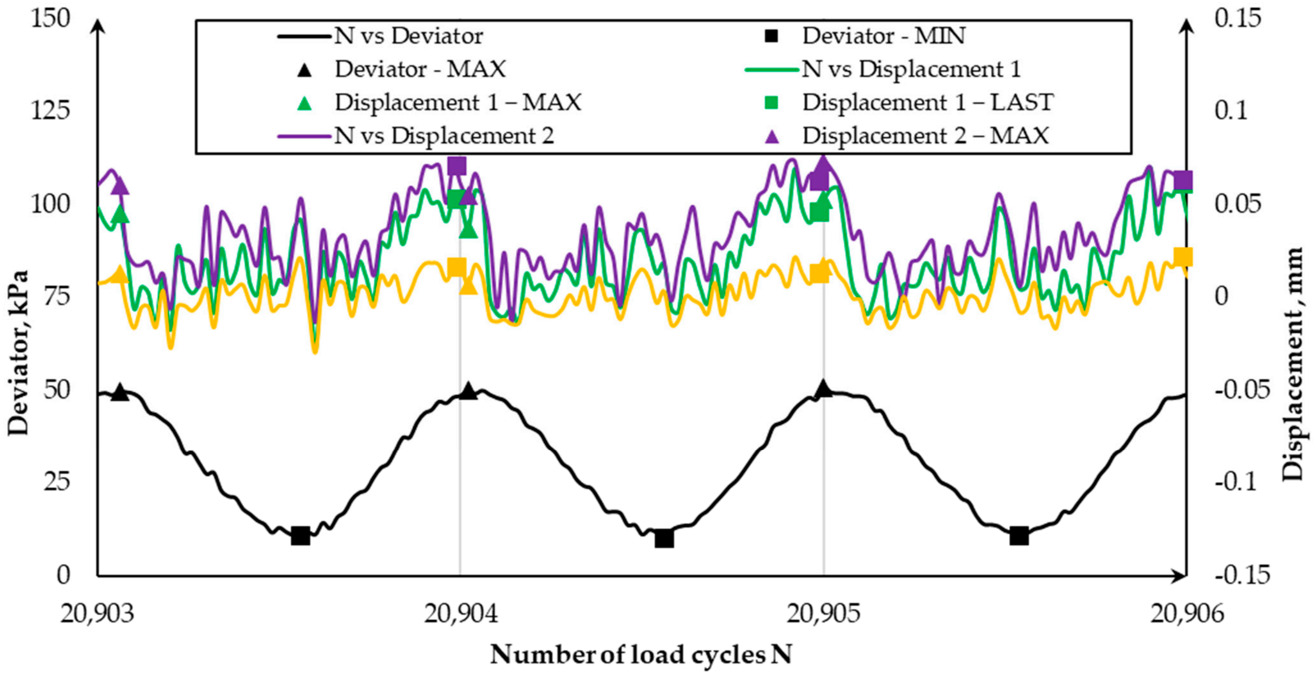

Figure 3. Fragment of results in graphs from a cyclic triaxial test of soil specimens.

2.2. Materials

A total of six different samples were tested and classified according to the LST 1331:2022 [19] standard: three as variously graded sands (SP) and three as well-graded sands (SG). Particle size distribution curves are provided in Figure 4.

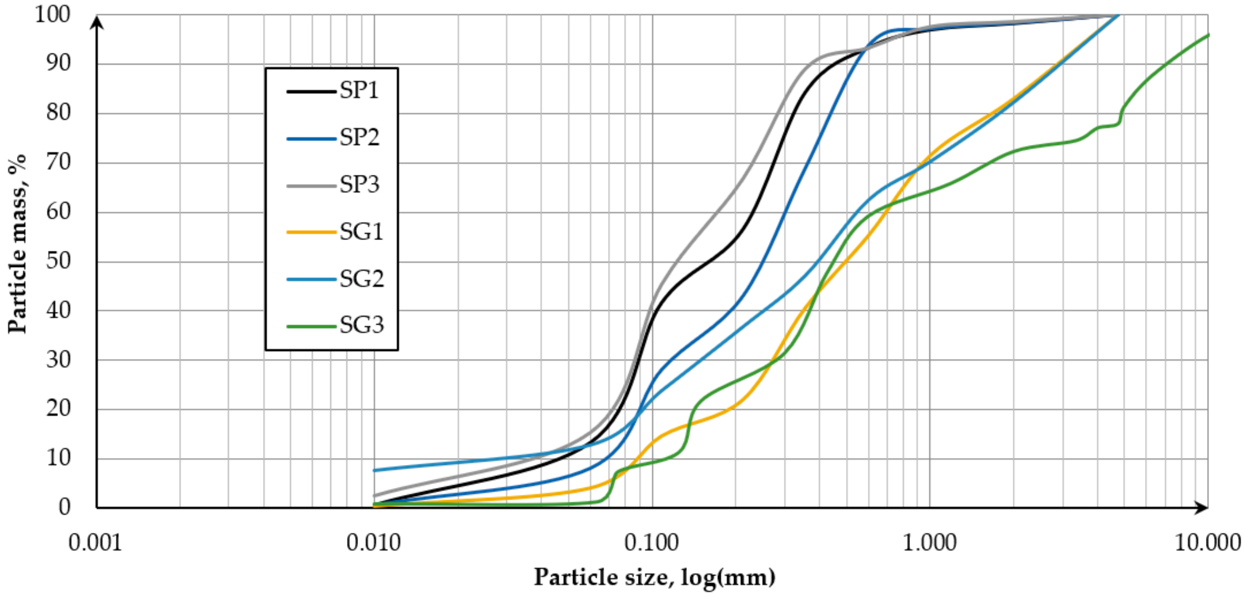

Figure 4. Particle size distribution curves of soils under discussion.

Classification of all samples according to LST 1331:2022 [19] and the Unified Soil Classification System (USCS) [20] is presented in Table 1, as well as uniformity coefficients (C_u) and coefficient of curvature (C_c). The density of each specimen was controlled at 100±5% dry density.

Table 1. Classification of specimens according to LST 1331:2022 and USCS.

Name of Specimen	C_u	C_c	Soil Classification	
			LST 1331:2022	USCS
SP1	4.90	0.72	Variously graded sand (SP)	Silty sand (SM)
SP2	4.74	0.75	Variously graded sand (SP)	Poorly graded sand (SP)
SP3	4.60	0.99	Variously graded sand (SP)	Silty sand (SM)
SG1	8.29	1.21	Well-graded sand (SG)	Well-graded sand (SW)
SG2	17.69	1.39	Well-graded sand (SG)	Well-graded sand (SW)
SG3	6.23	1.07	Well-graded sand (SG)	Well-graded sand (SW)

2.3. Models

Many different models were developed to predict the resilient modulus of coarse soils, which were based on the states of stresses and the physical and mechanical properties of the soil [21–23]. In this study, the authors have used four main models which are based on the stress state of the soil.

One of the most well-known models is a model developed by Hicks and Monismith [24–26], also known as the K-θ model, presented below:

$$E_r = K_1\,(\theta)^{K2} \tag{2}$$

where K_1 and K_2 are fitting parameters or regression coefficients, and θ is bulk stress which equals the sum of major σ_1, minor σ_3, and intermediate σ_2 stresses.

Another widely used model is that developed by Rahim and George [27,28], which incorporates deviatoric stress (σ_1) and atmospheric pressure (P_a) into the equation:

$$E_r = K_1 P_a \left(\frac{\Theta}{(\sigma_d + 1)} + 1 \right)^{K_2} \tag{3}$$

Uzan [29,30] proposed a model that incorporates octahedral shear stress (τ_{oct}):

$$E_r = K_1 P_a \left(\frac{\Theta}{P_a} \right)^{K_2} \left(\frac{\tau_{oct}}{P_a} \right)^{K_3} \tag{4}$$

octahedral shear stress (τ_{oct}) equal to ($\sqrt{2/3}$)($\sigma 1 - \sigma 3$), and K_3, same as K_1 and K_2, fitting parameters or regression coefficients.

Similar to Uzan's model is the Universal Witczak [31,32] model:

$$E_r = K_1 P_a \left(\frac{\Theta}{P_a} \right)^{K_2} \left(\frac{\tau_{oct}}{P_a} + 1 \right)^{K_3} \tag{5}$$

3. Results and Discussion

3.1. Test Results

After performing unconsolidated unsaturated drained cyclic triaxial tests, resilient modulus (E_r) values were obtained, which are shown in Figure 5. Received values directly depended on the confining pressure and deviatoric stress values used during the test, which are presented in the test program in Figure 1.

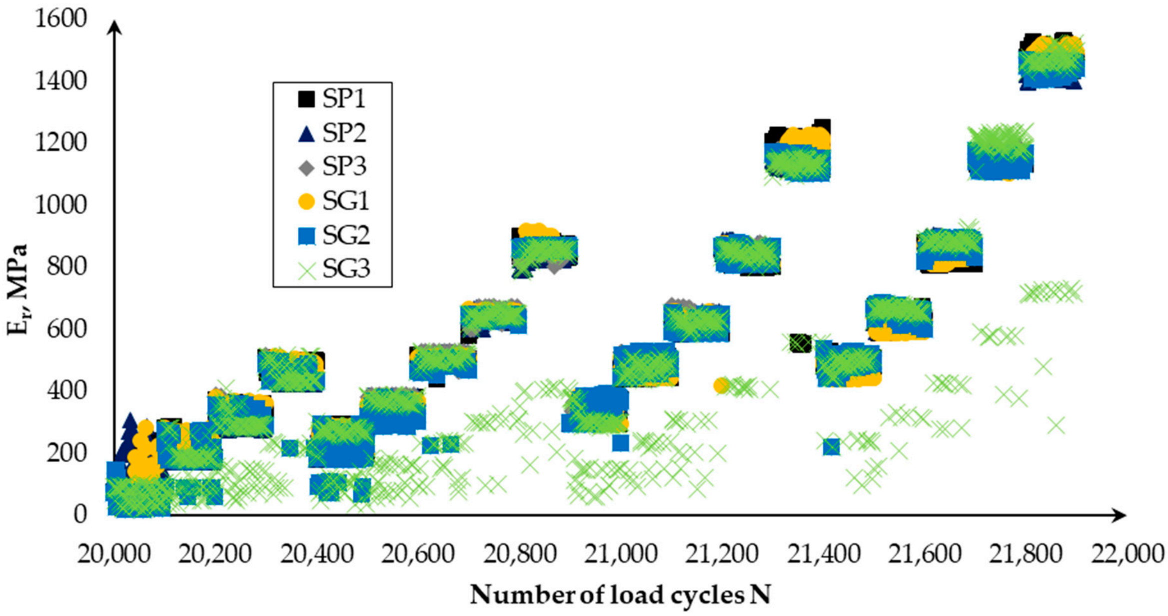

Figure 5. Obtained values of resilient modulus at a certain number of cycles.

3.2. Modeling Results

After obtaining the resilient modulus (E_r) values, using the previously listed models in formulae 2–5 to predict the resilient modulus, modeling was performed using the nonlinear generalized reduced gradient method to determine the average regression coefficients (K_n) and coefficients of determination (R^2) for every 100 cycles. The results of modeling for every specimen are provided in Tables 2–7.

Table 2. Determination of models' average regression coefficients for specimen SP1.

Start Cycle	No. of Cycles	σ_d	σ_3	K-θ		Rahim and George		Uzan			Universal Witczak		
				K_1	K_2	K_1	K_2	K_1	K_2	K_3	K_1	K_2	K_3
20,100	100	20.21	20.13	0.79	1.07	0.40	0.46	1.33	0.76	0.18	0.97	1.02	0.99
20,200	100	34.98	20.41	0.96	1.17	0.73	0.76	2.16	0.86	0.03	1.78	0.94	1.12
20,300	100	49.81	21.06	1.03	1.23	1.01	1.01	3.02	1.21	0.03	2.29	1.10	1.30
20,400	100	69.13	22.13	1.05	1.25	1.23	1.25	3.08	1.67	0.04	2.21	1.36	1.43
20,500	100	35.01	35.41	0.91	1.12	0.73	0.73	1.69	1.27	0.09	1.44	1.10	1.05
20,600	100	49.91	35.45	0.99	1.16	0.92	0.92	1.95	1.50	0.11	1.61	1.22	1.11
20,700	100	69.61	35.63	1.04	1.20	1.14	1.18	2.21	1.82	0.39	1.68	1.41	1.22
20,800	100	89.22	35.79	1.04	1.22	1.30	1.37	2.13	1.89	0.81	1.63	1.45	1.25
20,900	100	116.99	38.56	1.04	1.24	1.52	1.61	1.87	1.72	1.14	1.54	1.46	1.26
21,000	100	49.89	50.30	0.99	1.09	0.85	0.81	1.63	1.49	0.47	1.19	1.12	1.04
21,100	100	69.84	50.07	1.02	1.13	1.02	1.03	1.72	1.58	0.71	1.28	1.22	1.08
21,200	100	89.61	49.98	1.03	1.16	1.18	1.23	1.64	1.63	0.90	1.33	1.29	1.12
21,300	100	118.98	50.11	1.03	1.20	1.40	1.49	1.53	1.56	1.09	1.33	1.35	1.16
21,400	100	155.95	53.27	1.02	1.23	1.60	1.80	1.38	1.47	1.19	1.30	1.38	1.19
21,500	100	70.02	69.80	1.02	1.09	0.98	0.97	1.45	1.46	0.82	1.12	1.12	1.03
21,600	100	89.70	70.44	1.02	1.12	1.11	1.16	1.42	1.47	0.94	1.18	1.19	1.06
21,700	100	119.53	69.81	1.02	1.14	1.28	1.37	1.32	1.38	1.05	1.18	1.21	1.08
21,800	100	158.75	69.91	1.03	1.19	1.51	1.68	1.25	1.34	1.12	1.20	1.27	1.12
21,900	100	196.49	71.60	1.04	1.21	1.77	1.90	1.20	1.29	1.14	1.20	1.29	1.14
R^2				0.983835		0.984907		0.984669			0.984817		

Table 3. Determination of models' average regression coefficients for specimen SP2.

Start Cycle	No. of Cycles	σ_d	σ_3	K-θ		Rahim and George		Uzan			Universal Witczak		
				K_1	K_2	K_1	K_2	K_1	K_2	K_3	K_1	K_2	K_3
20,100	100	19.67	20.70	1.02	1.08	0.54	0.50	1.75	0.76	0.13	1.43	0.90	1.04
20,200	100	34.42	20.57	1.02	1.16	0.73	0.76	2.16	0.88	0.02	1.80	0.93	1.13
20,300	100	49.25	20.58	1.04	1.21	0.97	0.97	2.82	1.18	0.03	2.16	1.08	1.24
20,400	100	69.39	20.73	1.05	1.25	1.22	1.24	3.04	1.65	0.01	2.19	1.35	1.42
20,500	100	34.74	35.71	1.03	1.13	0.81	0.75	1.86	1.29	0.02	1.60	1.18	1.09
20,600	100	49.66	35.76	1.03	1.17	0.97	0.95	2.06	1.52	0.07	1.71	1.29	1.15
20,700	100	69.73	35.76	1.04	1.20	1.15	1.19	2.22	1.83	0.39	1.69	1.42	1.22
20,800	100	89.55	35.78	1.04	1.22	1.31	1.38	2.13	1.89	0.81	1.63	1.46	1.25
20,900	100	119.19	35.73	1.04	1.24	1.52	1.61	1.85	1.69	1.14	1.53	1.45	1.26
21,000	100	49.88	50.75	1.01	1.10	0.88	0.83	1.65	1.51	0.45	1.23	1.15	1.05
21,100	100	69.81	51.11	1.03	1.15	1.06	1.08	1.78	1.65	0.67	1.34	1.28	1.10
21,200	100	89.70	50.75	1.03	1.17	1.20	1.26	1.67	1.67	0.90	1.35	1.32	1.13
21,300	100	119.44	51.21	1.04	1.20	1.42	1.52	1.54	1.58	1.09	1.35	1.37	1.17
21,400	100	159.00	50.89	1.04	1.22	1.63	1.79	1.38	1.42	1.17	1.30	1.36	1.18
21,500	100	69.92	70.74	1.02	1.10	1.00	0.99	1.47	1.50	0.81	1.15	1.15	1.04
21,600	100	89.81	70.91	1.02	1.13	1.12	1.18	1.44	1.50	0.94	1.19	1.21	1.07
21,700	100	119.79	71.20	1.03	1.16	1.32	1.42	1.36	1.43	1.06	1.21	1.26	1.10
21,800	100	159.53	70.92	1.03	1.19	1.51	1.69	1.25	1.34	1.12	1.20	1.27	1.12
21,900	100	198.92	71.31	1.03	1.20	1.76	1.87	1.18	1.26	1.12	1.18	1.26	1.12
R^2				0.995557		0.995565		0.995525			0.995596		

Table 4. Determination of models' average regression coefficients for specimen SP3.

Start Cycle	No. of Cycles	σ_d	σ_3	K-θ		Rahim and George		Uzan			Universal Witczak		
				K_1	K_2	K_1	K_2	K_1	K_2	K_3	K_1	K_2	K_3
20,100	100	20.06	19.92	1.00	0.98	0.38	0.39	1.40	0.89	0.28	0.84	1.04	0.99
20,200	100	34.74	20.06	1.03	1.14	0.71	0.73	1.96	0.91	0.00	1.67	0.95	1.10
20,300	100	49.84	20.28	1.04	1.21	0.97	0.97	2.74	1.16	0.00	2.13	1.08	1.23
20,400	100	69.53	20.20	1.05	1.24	1.21	1.22	2.98	1.61	0.02	2.14	1.33	1.39
20,500	100	34.91	35.68	1.03	1.13	0.81	0.76	1.85	1.28	0.02	1.60	1.18	1.09
20,600	100	49.83	35.74	1.03	1.17	0.97	0.96	2.07	1.52	0.06	1.71	1.29	1.15
20,700	100	69.60	35.68	1.04	1.20	1.15	1.19	2.22	1.83	0.38	1.69	1.42	1.22
20,800	100	89.55	35.68	1.04	1.22	1.31	1.38	2.13	1.89	0.81	1.63	1.46	1.25
20,900	100	119.55	35.56	1.04	1.24	1.53	1.61	1.86	1.70	1.14	1.54	1.46	1.26
21,000	100	49.88	50.90	1.02	1.10	0.89	0.83	1.66	1.52	0.44	1.24	1.16	1.05
21,100	100	69.86	50.88	1.03	1.14	1.05	1.07	1.77	1.64	0.68	1.33	1.27	1.10
21,200	100	89.70	51.16	1.03	1.17	1.21	1.28	1.68	1.69	0.89	1.37	1.33	1.14
21,300	100	119.74	50.79	1.04	1.20	1.41	1.51	1.53	1.57	1.09	1.34	1.36	1.16
21,400	100	159.51	50.80	1.04	1.22	1.63	1.79	1.38	1.42	1.17	1.30	1.36	1.18
21,500	100	69.95	70.69	1.02	1.10	0.99	0.99	1.47	1.50	0.81	1.15	1.15	1.04
21,600	100	89.92	71.23	1.02	1.13	1.13	1.19	1.44	1.50	0.94	1.20	1.22	1.07
21,700	100	119.84	70.90	1.03	1.16	1.31	1.41	1.36	1.42	1.06	1.21	1.25	1.09
21,800	100	159.55	71.21	1.03	1.19	1.52	1.69	1.25	1.34	1.12	1.21	1.27	1.12
21,900	100	199.62	70.94	1.03	1.21	1.76	1.88	1.18	1.26	1.12	1.18	1.26	1.12
R^2				0.997692		0.997666		0.997671			0.997683		

Table 5. Determination of models' average regression coefficients for specimen SG1.

Start Cycle	No. of Cycles	σ_d	σ_3	K-θ		Rahim and George		Uzan			Universal Witczak		
				K_1	K_2	K_1	K_2	K_1	K_2	K_3	K_1	K_2	K_3
20,100	100	20.11	20.04	0.65	1.04	0.31	0.41	1.10	0.78	0.29	0.72	1.10	0.97
20,200	100	34.71	20.29	0.87	1.18	0.68	0.74	2.01	0.87	0.05	1.65	0.96	1.08
20,300	100	50.01	20.25	0.96	1.22	0.97	0.97	2.84	1.18	0.06	2.13	1.07	1.22
20,400	100	69.92	20.29	1.04	1.24	1.20	1.23	3.00	1.63	0.06	2.14	1.33	1.39
20,500	100	35.07	35.36	3.07	1.12	0.65	0.72	1.51	1.27	0.08	1.28	1.05	1.03
20,600	100	50.06	35.38	0.95	1.16	0.88	0.91	1.86	1.50	0.11	1.55	1.18	1.09
20,700	100	70.00	35.64	1.03	1.19	1.12	1.16	2.17	1.79	0.42	1.63	1.39	1.21
20,800	100	89.84	35.68	1.04	1.22	1.31	1.38	2.13	1.89	0.81	1.63	1.46	1.25
20,900	100	119.85	35.68	1.04	1.24	1.54	1.63	1.87	1.72	1.14	1.55	1.47	1.27
21,000	100	50.16	50.91	0.99	1.11	0.89	0.84	1.66	1.53	0.43	1.25	1.17	1.05
21,100	100	70.09	50.95	1.02	1.14	1.05	1.08	1.76	1.64	0.68	1.33	1.27	1.10
21,200	100	89.92	50.29	1.03	1.16	1.19	1.24	1.65	1.64	0.90	1.33	1.30	1.12
21,300	100	119.88	50.51	1.03	1.20	1.40	1.50	1.53	1.56	1.09	1.33	1.35	1.16
21,400	100	159.86	50.91	1.01	1.23	1.63	1.79	1.38	1.42	1.17	1.29	1.37	1.18
21,500	100	70.14	70.58	0.99	1.07	0.96	0.97	1.41	1.46	0.83	1.11	1.11	1.03
21,600	100	90.08	71.13	1.02	1.13	1.13	1.19	1.44	1.50	0.94	1.20	1.21	1.07
21,700	100	119.93	70.98	9.72	1.15	1.31	1.42	1.36	1.43	1.06	1.27	1.24	1.09
21,800	100	160.02	70.42	1.03	1.18	1.51	1.67	1.24	1.32	1.11	1.20	1.26	1.11
21,900	100	199.62	70.71	1.03	1.20	1.76	1.87	1.18	1.25	1.12	1.18	1.26	1.12
R^2				0.244736		0.991775		0.991805			0.991622		

Table 6. Determination of models' average regression coefficients for specimen SG2.

Start Cycle	No. of Cycles	σ_d	σ_3	K-θ		Rahim and George		Uzan			Universal Witczak		
				K_1	K_2	K_1	K_2	K_1	K_2	K_3	K_1	K_2	K_3
20,100	100	20.23	20.32	0.78	1.09	0.43	0.47	1.39	0.74	0.16	1.07	1.01	1.00
20,200	100	34.90	20.38	0.92	1.18	0.73	0.76	2.16	0.87	0.04	1.77	0.95	1.11
20,300	100	49.98	20.53	0.99	1.23	0.99	0.99	2.92	1.20	0.04	2.21	1.09	1.26
20,400	100	69.82	21.03	1.05	1.26	1.25	1.27	3.12	1.71	0.01	2.24	1.38	1.45
20,500	100	35.17	35.50	3.34	1.13	0.74	0.74	1.70	1.28	0.06	1.45	1.09	1.05
20,600	100	50.01	35.51	0.98	1.17	0.94	0.93	2.00	1.50	0.10	1.64	1.23	1.12
20,700	100	69.90	35.69	1.04	1.20	1.15	1.18	2.22	1.83	0.39	1.68	1.42	1.22
20,800	100	89.82	35.74	1.04	1.22	1.31	1.39	2.13	1.90	0.81	1.64	1.46	1.25
20,900	100	119.51	36.04	1.04	1.24	1.54	1.63	1.87	1.72	1.14	1.55	1.48	1.27
21,000	100	50.02	50.27	0.95	1.10	0.84	0.81	1.61	1.48	0.49	1.17	1.11	1.03
21,100	100	69.88	50.44	1.02	1.14	1.03	1.05	1.75	1.61	0.70	1.30	1.24	1.09
21,200	100	89.81	50.38	1.03	1.17	1.19	1.25	1.66	1.65	0.90	1.34	1.30	1.12
21,300	100	119.75	50.37	1.03	1.19	1.40	1.50	1.52	1.55	1.09	1.33	1.34	1.16
21,400	100	159.38	51.40	1.02	1.24	1.65	1.83	1.40	1.46	1.18	1.31	1.40	1.20
21,500	100	69.88	70.03	1.01	1.09	0.97	0.96	1.44	1.46	0.83	1.11	1.11	1.03
21,600	100	89.94	70.34	1.02	1.12	1.11	1.16	1.41	1.46	0.94	1.17	1.18	1.06
21,700	100	119.82	70.48	9.13	1.15	1.30	1.40	1.35	1.41	1.05	1.25	1.22	1.08
21,800	100	159.64	70.57	1.03	1.19	1.51	1.68	1.24	1.33	1.11	1.20	1.26	1.11
21,900	100	199.34	70.84	1.04	1.21	1.77	1.90	1.19	1.27	1.13	1.20	1.28	1.13
R^2				0.234674		0.994574		0.994593			0.994436		

Table 7. Determination of models' average regression coefficients for specimen SG3.

Start Cycle	No. of Cycles	σ_d	σ_3	K-θ		Rahim and George		Uzan			Universal Witczak		
				K_1	K_2	K_1	K_2	K_1	K_2	K_3	K_1	K_2	K_3
20,100	100	21.18	19.94	0.61	1.01	0.32	0.41	1.13	0.82	0.51	0.73	1.09	0.97
20,200	100	34.91	20.40	0.76	1.16	0.58	0.71	1.79	0.88	0.15	1.39	0.98	1.03
20,300	100	49.65	20.32	0.83	1.20	0.81	0.93	2.44	1.17	0.19	1.77	1.06	1.17
20,400	100	69.70	20.65	0.96	1.23	1.09	1.22	2.81	1.56	0.20	1.95	1.31	1.37
20,500	100	35.49	35.62	3.49	1.12	0.68	0.71	1.58	1.26	0.12	1.32	1.08	1.04
20,600	100	50.51	35.63	0.83	1.14	0.78	0.91	1.70	1.46	0.19	1.39	1.18	1.09
20,700	100	70.05	35.70	0.91	1.18	0.98	1.15	1.94	1.70	0.48	1.42	1.37	1.20
20,800	100	89.57	35.75	0.99	1.21	1.22	1.37	1.98	1.86	0.82	1.51	1.45	1.24
20,900	100	119.07	35.77	0.99	1.23	1.42	1.58	1.72	1.68	1.14	1.43	1.43	1.24
21,000	100	50.37	49.76	0.78	1.01	0.68	0.73	1.34	1.32	0.65	0.95	1.01	1.00
21,100	100	70.17	50.61	0.92	1.09	0.91	1.01	1.53	1.54	0.74	1.15	1.17	1.06
21,200	100	90.01	50.74	0.95	1.14	1.08	1.22	1.50	1.60	0.91	1.22	1.27	1.11
21,300	100	119.80	50.87	0.99	1.19	1.32	1.50	1.43	1.56	1.09	1.26	1.34	1.16
21,400	100	159.56	50.86	1.00	1.22	1.58	1.78	1.34	1.41	1.17	1.25	1.36	1.18
21,500	100	70.23	70.54	0.87	0.99	0.83	0.89	1.23	1.33	0.88	0.96	1.02	1.00
21,600	100	90.12	71.26	1.00	1.13	1.09	1.18	1.39	1.49	0.94	1.16	1.21	1.07
21,700	100	120.09	71.32	9.72	1.05	1.14	1.28	1.18	1.29	1.04	1.11	1.11	1.04
21,800	100	159.61	70.99	0.97	1.18	1.46	1.68	1.21	1.32	1.11	1.16	1.26	1.11
21,900	100	199.78	71.17	0.93	1.17	1.59	1.79	1.07	1.20	1.09	1.06	1.21	1.10
R^2				0.221460		0.799531		0.800532			0.802060		

After the predictive modeling, it can be seen in Table 2 that all used models for specimen SP1—variously graded sand almost perfectly predicted the resilience modulus values. The coefficient of determination (R^2) values of all models were higher than 0.98. The regression coefficient K_1 used in the K-θ model (2) varied from 0.79 to 1.05 and regression coefficient K_2 varied from 1.07 to 1.25. The regression coefficient K_1 used in the Rahim and George model (3) varied from 0.40 to 1.77 and regression coefficient K_2 varied from 0.46 to 1.90. The regression coefficient K_1 used in the Uzan model (4) varied from 1.20 to 3.08, regression coefficient K_2 varied from 0.76 to 1.89, and regression coefficient K_3 varied from 0.03 to 1.19. The regression coefficient K_1 used in the Universal Witczak model (5) varied from 0.97 to 2.29, regression coefficient K_2 varied from 0.94 to 1.46, and regression coefficient K_3 varied from 0.99 to 1.43.

A similar situation is seen with specimen SP2—variously graded sand (Table 3), all used models almost perfectly predicted the resilience modulus values, and the coefficient of determination (R^2) values of all models were higher than 0.99. The regression coefficient K_1 used in the K-θ model (2) varied from 1.01 to 1.05 and regression coefficient K_2 varied from 1.08 to 1.25. The regression coefficient K_1 used in the Rahim and George model (3) varied from 0.54 to 1.76 and regression coefficient K_2 varied from 0.50 to 1.87. The regression coefficient K_1 used in the Uzan model (4) varied from 1.18 to 3.04, regression coefficient K_2 varied from 0.76 to 1.89, and regression coefficient K_3 varied from 0.01 to 1.17. The regression coefficient K_1 used in the Universal Witczak model (5) varied from 1.15 to 2.19, regression coefficient K_2 varied from 0.90 to 1.46, and regression coefficient K_3 varied from 1.04 to 1.42.

For the specimen SP3—variously graded sand (Table 4), the coefficient of determination (R^2) values of all models were higher than 0.99 also. The regression coefficient K_1 used in the K-θ model (2) varied from 1.00 to 1.05 and regression coefficient K_2 varied from 0.98 to 1.24. The regression coefficient K_1 used in the Rahim and George model (3) varied from 0.38 to 1.76 and regression coefficient K_2 varied from 0.39 to 1.88. The regression coefficient K_1 used in the Uzan model (4) varied from 1.18 to 2.98, regression coefficient K_2 varied from 0.89 to 1.89, and regression coefficient K_3 varied from 0 to 1.17. The regression coefficient K_1 used in the Universal Witczak model (5) varied from 0.84 to 2.14, regression coefficient K_2 varied from 0.95 to 1.46, and regression coefficient K_3 varied from 0.99 to 1.39.

For the specimen SG1—well-graded sand (Table 5), the coefficient of determination (R^2) value using the K-θ model (2) is 0.24. Other used models almost perfectly predicted the resilience modulus values and the value coefficients of determination (R^2) for the rest of the models were higher than 0.99. The regression coefficient K_1 used in the K-θ model (2) varied from 0.65 to 9.72 and regression coefficient K_2 varied from 1.04 to 1.24. The regression coefficient K_1 used in the Rahim and George model (3) varied from 0.31 to 1.76 and regression coefficient K_2 varied from 0.41 to 1.87. The regression coefficient K_1 used in the Uzan model (4) varied from 1.10 to 3.00, regression coefficient K_2 varied from 0.78 to 1.89, and regression coefficient K_3 varied from 0.05 to 1.17. The regression coefficient K_1 used in the Universal Witczak model (5) varied from 0.72 to 2.14, regression coefficient K_2 varied from 0.96 to 1.47, and regression coefficient K_3 varied from 0.97 to 1.39.

For the specimen SG2—well-graded sand (Table 6), the coefficient of determination (R^2) value using the K-θ model (2) is 0.22. Other used models almost perfectly predicted the resilience modulus values. The value coefficients of determination (R^2) for the rest of the models were higher than 0.99. The regression coefficient K_1 used in the K-θ model (2) varied from 0.78 to 9.13 and regression coefficient K_2 varied from 1.09 to 1.26. The regression coefficient K_1 used in the Rahim and George model (3) varied from 0.43 to 1.77 and regression coefficient K_2 varied from 0.47 to 1.90. The regression coefficient K_1 used in the Uzan model (4) varied from 1.19 to 3.12, regression coefficient K_2 varied from 0.74 to 1.90, and regression coefficient K_3 varied from 0.01 to 1.18. The regression coefficient K_1 used in the Universal Witczak model (5) varied from 1.07 to 2.24, regression coefficient K_2 varied from 0.95 to 1.48, and regression coefficient K_3 varied from 1.00 to 1.45.

For the specimen SG3—well-graded sand (Table 7), the coefficient of determination (R^2) value using the K-θ model (2) is 0.22. The regression coefficient K_1 varied from 0.61 to 9.72 and regression coefficient K_2 varied from 0.99 to 1.23. The coefficient of determination (R^2) value used in the Rahim and George model (3) is 0.80, the regression coefficient K_1 varied from 0.32 to 1.59, and regression coefficient K_2 varied from 0.41 to 1.79. The coefficient of determination (R^2) value used in the Uzan model (4) is 0.80, the regression coefficient K_1 varied from 1.07 to 2.81, the regression coefficient K_2 varied from 0.82 to 1.86, and the regression coefficient K_3 varied from 0.12 to 1.17. The coefficient of determination (R^2) value used in the Universal Witczak model (5) is 0.80, the regression coefficient K_1 varied from 0.73 to 1.95, regression coefficient K_2 varied from 0.98 to 1.45, and the regression coefficient K_3 varied from 0.97 to 1.37.

3.3. Proposed Model

The values of regression coefficients (K_n) for all used predictive models strongly fluctuate at different deviatoric stresses and confining stresses (Tables 2–7). Therefore, to accurately predict the resilient modulus of test specimens, large-scale data tables should be used, meaning that regression coefficients (K_n) need to be determined using specific deviatoric and confining stresses. To avoid this, a new, simpler model was searched for, which would help make resilient modulus predictions with sufficient accuracy.

The models for predicting the resilient modulus presented in the Materials and Methods chapter were based on three main stress variables—deviatoric stress, bulk stresses, and octahedral stress. The power dependence of the resilient modulus on the bulk stress is presented in Figure 6. Power dependence, compared to linear, exponential, logarithmic, and 2nd order polynomials, best predicted the fit of values for the dependence of the resilient modulus on bulk stress.

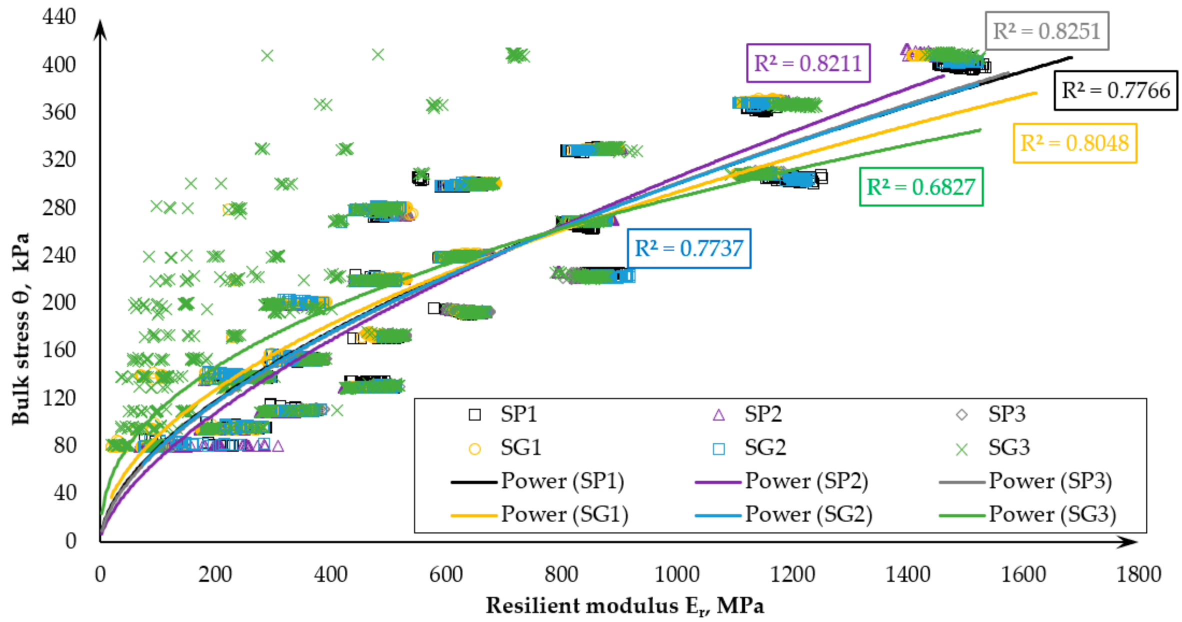

Figure 6. Resilient modulus correlation with bulk stress.

The linear dependence of the resilient modulus on octahedral stress is presented in Figure 7. Linear dependence, compared to power, exponential, logarithmic, and 2nd order polynomial, best predicted the fit of values for the dependence of the resilient modulus on octahedral stress.

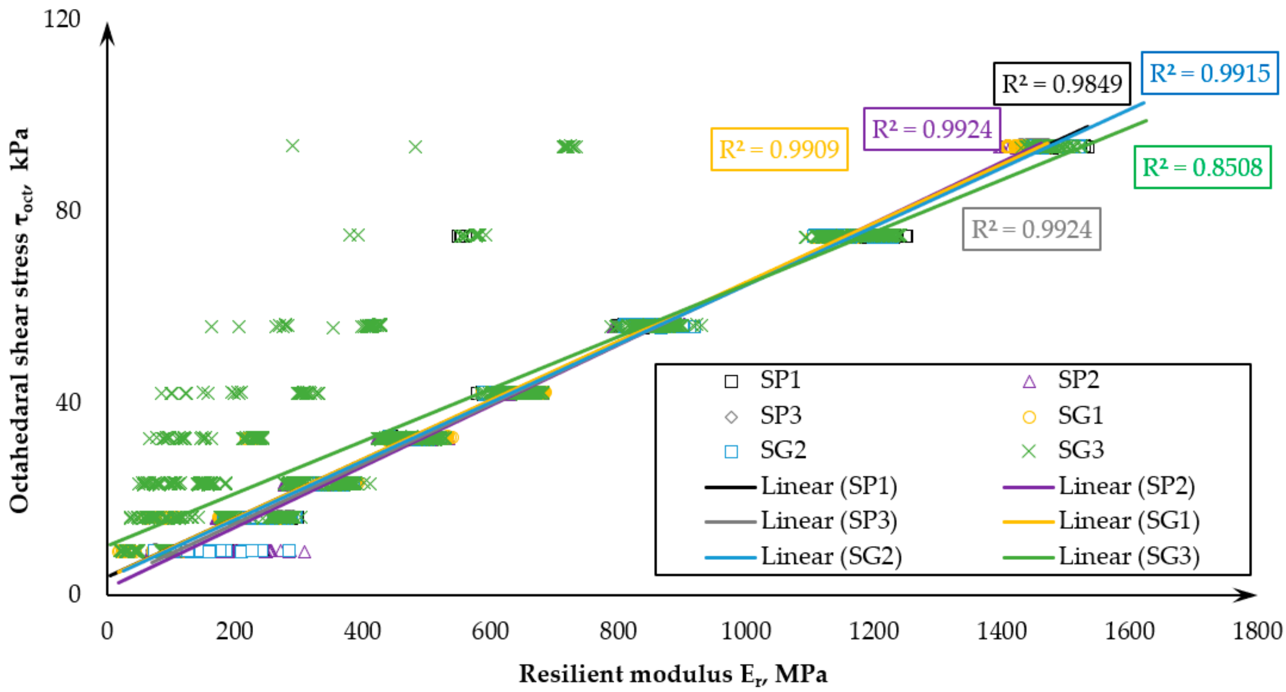

Figure 7. Resilient modulus correlation with octahedral shear stress.

As can be seen from Figures 6 and 7, the linear dependence of the resilient modulus on octahedral stress had a coefficient of determination from 0.85 to 0.99, while the power dependence of the resilient modulus on the bulk stress had a coefficient of determination only from 0.68 to 0.83. Based on these results, the authors of the paper propose the following Octahedral Shear Stress (OSS) prediction model:

$$E_r = K_1\ \tau_{oct} - K_2 \tag{6}$$

where K_1 and K_2 are regression coefficients which are provided for every tested specimen separately in Table 8.

Table 8. The OSS models' regression coefficients for specimens.

Name of Specimen	Soil Classification		OSS Model ($E_R = K_1\ \tau_{oct} - K_2$)		
	LST 1331:2022	USCS	K_1	K_2	R^2
SP1	Variously graded sand (SP)	Silty sand (SM)	16.08	53.90	0.98
SP2	Variously graded sand (SP)	Poorly graded sand (SP)	15.60	19.46	0.99
SP3	Variously graded sand (SP)	Silty sand (SM)	15.91	37.24	0.85
SG1	Well-graded sand (SG)	Well-graded sand (SW)	16.09	56.29	0.99
SG2	Well-graded sand (SG)	Well-graded sand (SW)	16.24	55.74	0.99
SG3	Well-graded sand (SG)	Well-graded sand (SW)	15.58	77.73	0.85

4. Conclusions

After the determination of the resilient modulus values of variously graded sands (SP1, SP2, SP3) and well-graded sand (SG1, SG2, SG3), and predictive modeling using the models reviewed in the Materials and Methods chapter, the following conclusions can be drawn:

- Using the K-θ model developed by Hicks and Monismith to predict resilient modulus, the coefficient of determination (R^2) value using determined regression coefficients provided in Tables 2–7 ranges from 0.22 to 0.99;

- Using the Rahim and George model to predict resilient modulus, the coefficient of determination (R^2) value using determined regression coefficients provided in Tables 2–7 ranges from 0.80 to 0.99;
- Using the Uzan model to predict resilient modulus, the coefficient of determination (R^2) value using determined regression coefficients provided in Tables 2–7 ranges from 0.80 to 0.99;
- Using the Universal Witczak model to predict resilient modulus, the coefficient of determination (R^2) value using determined regression coefficients provided in Tables 2–7 ranges from 0.80 to 0.99;
- The Octahedral Shear Stress model, proposed by the authors of the paper, predicts the resilient modulus with a coefficient of determination (R^2) ranging from 0.85 to 0.99, using regression coefficients provided in Table 8. The advantage of the model is the use of small-scale data tables, meaning that fixed K_1 and K_2 regression coefficients can be assigned to a specific specimen type without the need to determine them using specific deviatoric and confining stresses. Additional investigation of the regression coefficient must be performed, separately taking into account different stress states of specimen to avoid overfitting as much as possible.

Authors hope that more advanced laboratory testing such as cyclic triaxial testing will be performed to derive more accurate prediction models or to calibrate existing models for the determination of the resilient modulus. Wider use of a resilient modulus determined by prediction models could potentially help to design road structures more accurately while saving time and expenditures.

Author Contributions: Conceptualization and methodology, T.T. and Š.S.; formal analysis, investigation, and data curation, T.T. and Š.S.; writing—original draft preparation T.T. and Š.S.; writing—review and editing, T.T. and Š.S. All authors have read and agreed to the published version of the manuscript.

Funding: This research received no external funding.

Data Availability Statement: The data presented in this study are available on request.

Conflicts of Interest: The authors declare no conflict of interest.

References

1. Transportation Officials. *Mechanistic-Empirical Pavement Design Guide: A Manual of Practice*; AASHTO: Washington, DC, USA, 2008.
2. *EN 13286-7*; Unbound and Hydraulically Bound Mixtures–Cyclic Load Triaxial Test for Unbound Mixtures. CEN: Brussels, Belgium, 2004.
3. Transportation Officials. *AASHTO Guide for Design of Pavement Structures*; AASHTO: Washington, DC, USA, 1993.
4. Kumar, P.; Puppala, A.J.; Tingle, J.S.; Chakraborty, S.; Sarat Chandra Congress, S. Resilient Characteristics of Polymer Emulsion-Treated Sandy Soil. *Transp. Res. Rec.* **2022**, *2676*, 526–538. [CrossRef]
5. Kim, S.S.; Pahno, S.; Durham, S.A.; Yang, J.; Chorzepa, M.G. *Prediction of Resilient Modulus from the Laboratory Testing of Sandy Soils*; Georgia Department of Transportation, Office of Performance-Based Management and Research: Atlanta, GA, USA, 2019.
6. Liu, X.; Zhang, X.; Wang, H.; Jiang, B. Laboratory testing and analysis of dynamic and static resilient modulus of subgrade soil under various influencing factors. *Constr. Build. Mater.* **2019**, *195*, 178–186. [CrossRef]
7. Ackah, F.S.; Zhuochen, N.; Huaiping, F. Effect of wetting and drying on the resilient modulus and permanent strain of a sandy clay by RLTT. *Int. J. Pavement Res. Technol.* **2021**, *14*, 366–377. [CrossRef]
8. Yaghoubi, E.; Yaghoubi, M.; Guerrieri, M.; Sudarsanan, N. Improving expansive clay subgrades using recycled glass: Resilient modulus characteristics and pavement performance. *Constr. Build. Mater.* **2021**, *302*, 124384. [CrossRef]
9. Tuan, N.A.; Chieu, P.Q. The Effect of Moisture and Fine Grain Content on the Resilient Modulus of Sandy Clay Embankment Roadbed. *Eng. Technol. Appl. Sci. Res.* **2021**, *11*, 7118–7124. [CrossRef]
10. Behiry, A.E.A.E.M. Fatigue and rutting lives in flexible pavement. *Ain Shams Eng. J.* **2012**, *3*, 367–374. [CrossRef]
11. Sas, W.; Głuchowski, A.; Soból, E.; Bąkowski, J.; Szymański, A. Analysis of the multistage cyclic loading test on resilient modulus value. *Ann. Wars. Univ. Life Sci.–SGGW-Land Reclam* **2016**, *48*, 53–65. [CrossRef]
12. Jin, M.S.; Lee, K.W.; Kovacs, W.D. Seasonal variation of resilient modulus of subgrade soils. *J. Transp. Eng.* **1994**, *120*, 603–616. [CrossRef]
13. Filotenkovas, V.; Vaitkus, A. Influence of the aggregate shape and resistance to fragmentation on unbound base layer resilient modulus. *Balt. J. Road Bridge Eng.* **2022**, *17*, 104–119. [CrossRef]

14. Titi, H.H.; Elias, M.B.; Helwany, S. *Determination of Typical Resilient Modulus Values for Selected Soils in Wisconsin*; Wisconsin Highway Research Program: Madison, WI, USA, 2006.
15. Tamošiūnas, T.; Žaržojus, G.; Skuodis, Š. Indirect determination of soil Young's modulus in Lithuania using cone penetration test data. *Balt. J. Road Brodge Eng.* **2022**, *17*, 1–24. [CrossRef]
16. Fathi, A.; Tirado, C.; Rocha, S.; Mazari, M.; Nazarian, S. A Machine-Learning Approach for Extracting Modulus of Compacted Unbound Aggregate Base and Subgrade Materials Using Intelligent Compaction Technology. *Infrastructures* **2021**, *6*, 142. [CrossRef]
17. Pahno, S.; Yang, J.J.; Kim, S.S. Use of machine learning algorithms to predict subgrade resilient modulus. *Infrastructures* **2021**, *6*, 78. [CrossRef]
18. Skuodis, Š.; Karpis, R.; Zakarka, M.; Gedvilas, M.; Raginis, V.; Orlova, K.; Katauskas, M. Grunto, veikiamo periodinėmis apkrovomis, elgsenos tyrimai. *Geol. Geogr.* **2018**, *4*, 159–167. [CrossRef]
19. *LST 1331*; Automobilių Kelių Gruntai. Klasifikacija [Soil for roads. Classification]. LSD: Vilnius, Lithuania, 2022.
20. Daryati, D.; Widiasanti, I.; Septiandini, E.; Ramadhan, M.A.; Sambowo, K.A.; Purnomo, A. Soil characteristics analysis based on the unified soil classification system. *J. Phys. Conf. Ser.* **2019**, *1402*, 022028. [CrossRef]
21. Zhang, J.; Peng, J.; Zeng, L.; Li, J.; Li, F. Rapid estimation of resilient modulus of subgrade soils using performance-related soil properties. *Int. J. Pavement Eng.* **2021**, *22*, 732–739. [CrossRef]
22. Zhang, J.; Peng, J.; Liu, W.; Lu, W. Predicting resilient modulus of fine-grained subgrade soils considering relative compaction and matric suction. *Road Mater. Pavement Des.* **2021**, *22*, 703–715. [CrossRef]
23. Hanandeh, S.; Ardah, A.; Abu-Farsakh, M. Using artificial neural network and genetics algorithm to estimate the resilient modulus for stabilized subgrade and propose new empirical formula. *Transp. Geotech.* **2020**, *24*, 100358. [CrossRef]
24. Hicks, R.G. *Factors Influencing the Resilient Properties of Granular Materials*; University of California, Berkeley: Berkeley, CA, USA, 1970.
25. Adomako, S.; Engelsen, C.J.; Thorstensen, R.T.; Barbieri, D.M. Repeated load triaxial testing of recycled excavation materials blended with recycled phyllite materials. *Materials* **2022**, *15*, 621. [CrossRef]
26. Chowdhury, S.R.M. Evaluation of resilient modulus constitutive equations for unbound coarse materials. *Constr. Build. Mater.* **2021**, *296*, 123688. [CrossRef]
27. Rahim, A.M.; George, K.P. Models to estimate subgrade resilient modulus for pavement design. *Int. J. Pavement Eng.* **2005**, *6*, 89–96. [CrossRef]
28. Fedakar, H.I. Developing New Empirical Formulae for the Resilient Modulus of Fine-Grained Subgrade Soils Using a Large Long-Term Pavement Performance Dataset and Artificial Neural Network Approach. *Transp. Res. Rec.* **2022**, *2676*, 58–75. [CrossRef]
29. Uzan, J. Characterization of granular material. *Transp. Res. Rec.* **1985**, *1022*, 52–59.
30. Ni, B.; Hopkins, T.C.; Sun, L.; Beckham, T.L. Modeling the resilient modulus of soils. In *Bearing Capacity of Roads, Railways and Airfields*; CRC Press: Boca Raton, FL, USA, 2020; pp. 1131–1142.
31. Yoder, E.J.; Witczak, M.W. Chapter 2: Stresses in flexible pavements. In *Principles of Pavement Design*; John Wiley and Sons Inc.: New York, NY, USA, 1975; pp. 24–76.
32. Al-Dulaimi, Y.F.; Awed, A.M.; Gabr, A.R.; El-Badawy, S.M. Predicting Resilient Modulus of Unbound Granular Base/Subbase Material.(Dept. C). *MEJ. Mansoura Eng. J.* **2022**, *47*, 1–10. [CrossRef]